LETTERS

Net production of oxygen in the subtropical ocean

Stephen C. Riser[1] & Kenneth S. Johnson[2]

The question of whether the plankton communities in low-nutrient regions of the ocean, comprising 80% of the global ocean surface area, are net producers or consumers of oxygen and fixed carbon is a key uncertainty in the global carbon cycle[1,2]. Direct measurements in bottle experiments indicate net oxygen consumption in the sunlit zone[3–6], whereas geochemical evidence suggests that the upper ocean is a net source of oxygen[2]. One possible resolution to this conflict is that primary production in the gyres is episodic[1,2,6] and thus difficult to observe: in this model, oligotrophic regions would be net consumers of oxygen during most of the year, but strong, brief events with high primary production rates might produce enough fixed carbon and dissolved oxygen to yield net production as an average over the annual cycle. Here we examine the balance of oxygen production over three years at sites in the North and South Pacific subtropical gyres using the new technique of oxygen sensors deployed on profiling floats. We find that mixing events during early winter homogenize the upper water column and cause low oxygen concentrations. Oxygen then increases below the mixed layer at a nearly constant rate that is similar to independent measures of net community production. This continuous oxygen increase is consistent with an ecosystem that is a net producer of fixed carbon (net autotrophic) throughout the year, with episodic events not required to sustain positive oxygen production.

The uncertainty over whether oligotrophic regions are net producers or consumers of oxygen has "profound implications for our understanding of the oceanic carbon cycle"[7]. However, the direct measurement of oxygen production and respiration in the oligotrophic ocean, which in principle could be used to resolve the question, is a difficult task. Rates of primary production and respiration are small, with each typically on the order of $1\,\mu mol\,O_2\,kg^{-1}\,d^{-1}$ (ref. 6). Net community production (NCP), which is equal to primary production minus respiration at all trophic levels, is even smaller and more difficult to measure.

We examine here the balance of oxygen production and consumption by using oxygen sensors deployed on two profiling floats[8] as part of the international Argo programme[9] (see Methods). Profiling floats use a buoyancy engine to ascend from a parking depth of 1,000 or 2,000 m every ten days, with oceanographic properties monitored on the ascent and transmitted to shore by satellite. Oxygen measurements are a recent addition to float capabilities[10,11]. Float 0894 collected measurements for three years in the vicinity of the Hawaii Ocean Time series (HOT) station (23° N, 158° W; Fig. 1a), whereas float 1326 collected profiles for 3 years near 22° S, 120° W in the South Pacific (Fig. 1b). Oxygen values are plotted against density in Fig. 1c, d for all profiles. The plots illustrate the repeatability of the oxygen measurement, which is $\pm 1.5\,\mu mol\,kg^{-1}$ (one standard deviation over 3 years; see Methods). These data are well suited to examining the oxygen balance of subtropical waters because of the relatively rapid ten-day sampling time, high stability and precision of the oxygen measurements, and the fact that these floats remained in nearly homogeneous regions of the ocean for an extended period.

The oxygen concentration and seawater density for the upper 200 m of the water column during the period that each float operated (Fig. 2) indicate that during the autumn of each year the upper 100 m of the water column at the HOT site and 150 m at 22° S undergo strong mixing, homogenizing oxygen and density (Fig. 2). Oxygen concentrations reach low and vertically uniform values during this
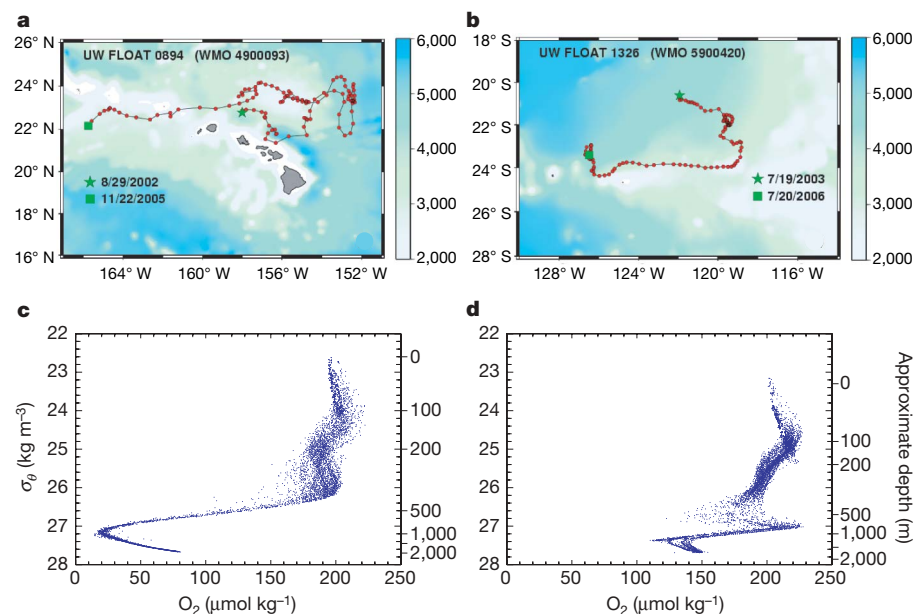

Figure 1 | Profile locations and oxygen concentration in the subtropical Pacific. a, b, Red dots show the locations of 112 vertical profiles measured by float 0894 in the North Pacific (**a**) and 104 vertical profiles measured by float 1326 in the South Pacific (**b**). Profiles were collected at ten-day intervals. A green star marks the first profile location (29 August 2002 in **a**; 19 July 2003 in **b**) and a green square shows the last profile location (22 November 2005 in **a**; 20 July 2006 in **b**) for each float. The colour bars indicate ocean depth (metres). **c, d,** Raw oxygen data from float 0894 (**c**) and float 1326 (**d**) as functions of potential density σ_θ and depth, where σ_θ is adiabatic density $- 1,000$. For float 0894, the trajectory is the complete trajectory from launch to the end of the float mission; in the analyses performed here, dissolved oxygen data are used only up to the first 100 profiles of float 0894, after which the oxygen sensor failed.

[1]School of Oceanography, University of Washington, Seattle, Washington 98195, USA. [2]Monterey Bay Aquarium Research Institute, Moss Landing, California 95039, USA.

brief period. For the remainder of each year, oxygen accumulates in the water trapped under the seasonal thermocline. This accumulation of oxygen produces a distinctive shallow oxygen maximum (SOM)[12].

There is a continuous increase with time in dissolved oxygen in the SOM layer after the autumn period of mixing (Fig. 3). The oxygen anomaly (oxygen concentration minus oxygen solubility) increases at nearly the same rate, indicating that the increase is not driven by solubility changes. The increase in oxygen concentration in the SOM cannot be produced by changes in mixing or solubility and must therefore be due to biological oxygen production, as proposed[12]. The rate of oxygen production was determined from the slopes of straight lines fitted by least squares to the oxygen concentration data from early winter to early autumn (about 300 days) for each year (the pink lines in Fig. 3). Annual NCP rates were estimated from these slopes at depths below the pycnocline by converting oxygen production to carbon uptake with the modified Redfield ratio (150 mol of O_2 produced per 106 mol of CO_2 fixed[13]) and then extrapolating to an annual value by multiplying the daily increase by 365 (Fig. 4).

The NCP shows a systematic increase from values not significantly different from zero at depths near the bottom of the euphotic zone (the 1% light level is near 115 m at the HOT site[14] and at about 150 m at 22° S) to maximum values at the base of the pycnocline. The highest slopes are equivalent to a NCP of about 15 mmol C m^{-3} yr^{-1} near Hawaii and about 7 mmol C m^{-3} yr^{-1} in the South Pacific gyre. Above the pycnocline, oxygen is lost to the atmosphere by gas exchange, and NCP cannot be reliably estimated from oxygen alone. The yearly cycles of dissolved inorganic carbon in the mixed layer at
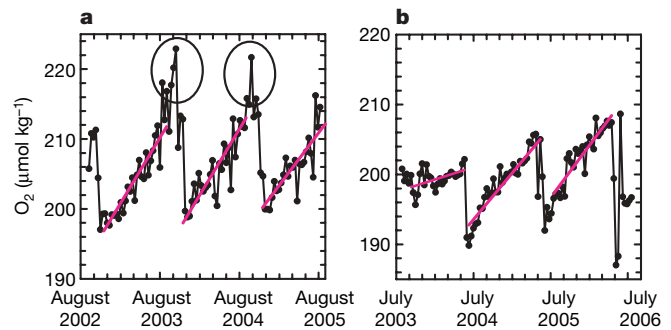
Figure 3 | Oxygen concentrations in the SOM versus time. Oxygen concentrations at 78 m for float 0894 (**a**) and 87 m for float 1326 (**b**) are shown. Black lines and solid circles are oxygen concentrations measured by the float at each depth. Pink lines are fitted to the oxygen data each year by least squares to estimate the rate of oxygen production. Large black ovals in **a** identify late summer blooms that increase oxygen concentration in the SOM significantly above the trend line predicted from data earlier in each year.

HOT (Fig. 1 in ref. 15) also have a continuous decrease at rates similar to that of oxygen production. Dissolved inorganic carbon then increases rapidly in the autumn, just as oxygen decreases. Given the similarity of oxygen and dissolved inorganic carbon cycles, the maximum rates at HOT of 15 mmol C m^{-3} yr^{-1} were extended through the mixed layer to give vertically integrated NCP values of 1.6 ± 0.2 mol C m^{-2} yr^{-1} (mean ± s.d.) (Fig. 4). Keeling *et al.*[15] summarized 11 reported measurements of NCP at the nearby HOT station that had a mean of 1.9 ± 0.6 mol C m^{-2} yr^{-1} (mean ± s.d.). However, Keeling *et al.*[15] reported seasonal variability in NCP that we do not observe. This must have been because they modelled a mean year obtained by averaging 14 years of observations, which obscured the constant rate of NCP.

The reasonable agreement of the NCP derived from float-based oxygen measurements with 11 previous estimates corroborates our hypothesis that the increase in oxygen measured by the floats is the result of biological oxygen production. We conclude that the quasi-lagrangian nature of the floats does not impart a significant bias in the
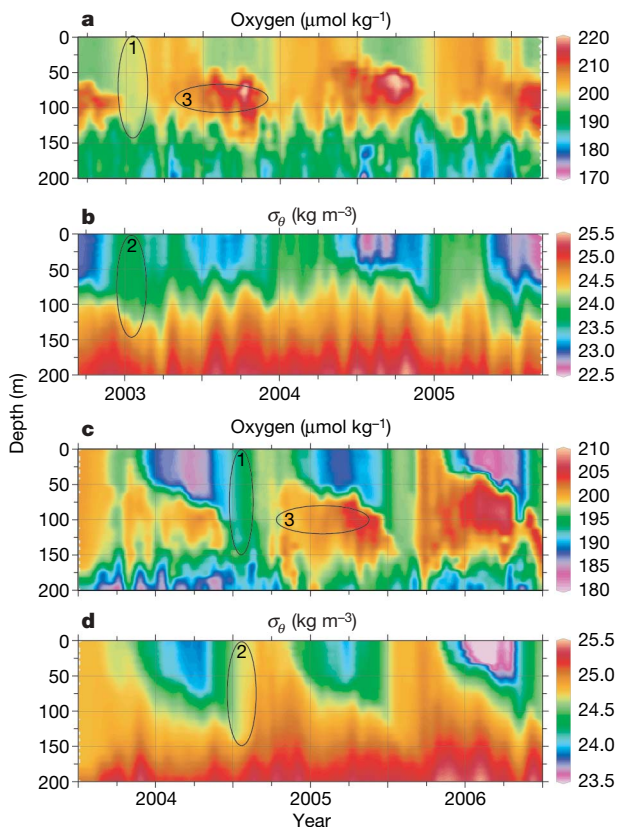
Figure 2 | Contours of the evolution of oxygen concentration and density in the upper 200 m. Oxygen (**a**, **c**) and potential density σ_θ (**b**, **d**) are shown during the three years that floats 0894 (**a**, **b**) and 1326 (**c**, **d**) operated. Contours were prepared with the program Ocean Data View[19]. Periods of convective overturn in 2003 (float 0894) and 2004 (float 1326), during which oxygen and density become vertically homogenous, are identified by ellipses labelled 1 and 2, respectively. The subsequent oxygen increase to form the SOM is identified by ellipses labelled 3.
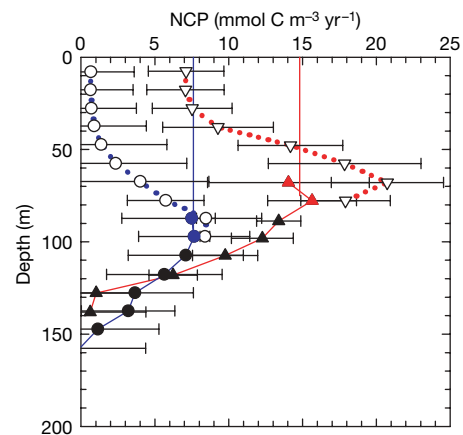
Figure 4 | Plot of NCP versus depth. Triangles show data for float 0894, and circles data for float 1326. Filled symbols were calculated from the slope of oxygen against time. Open symbols were calculated from the slope of oxygen anomaly (oxygen − oxygen solubility) against time in the mixed layer. Vertical solid lines are an extrapolation to the surface of the two highest rates (symbols coloured in red or blue) based on the slope of oxygen against time at each site. Oxygen production was converted to carbon units by using the modified Redfield ratio[13], as explained in the text. Vertically integrated NCP is the area to the left of the lines connecting filled symbols for each float and the solid line extending that data to the surface. Error bars (±1 s.d.) were computed from the rate of oxygen change for each of the three years for which the floats operated.

measured evolution of oxygen concentration. An estimate of NCP calculated from three years of oxygen data reported by float 1326 near 22° S ($0.9 \pm 0.4 \, \text{mol C m}^{-2} \text{yr}^{-1}$) is about one-half of the HOT value. It is not surprising that the calculated NCP near 22° S is smaller than that near Hawaii (Fig. 4), because float 1326 operated in a region that is considered to have one of the lowest rates of primary production in the world ocean[16].

The increase in dissolved oxygen beneath the pycnocline follows a relatively smooth trend over time (Fig. 3). Late summer blooms near the HOT site[17] are apparent in the float 0894 data set (Fig. 3a), but they only add to the already positive oxygen increase. The mean rate of increase in oxygen in the SOM near the HOT site is $0.5 \, \mu\text{mol kg}^{-1}$ every ten days, excluding the period of the late summer blooms. The observed changes in oxygen in the core of the SOM between each cycle of float 0894 in the months December to June have a frequency distribution that is not significantly different from a normal distribution with a mean of $0.5 \, \mu\text{mol kg}^{-1}$ and a standard deviation of $1.5 \, \mu\text{mol kg}^{-1}$ (Kolmogorov–Smirnov test; $P = 0.20$, 0.11 and 0.89 for 2003, 2004 and 2005, respectively). Such a distribution is consistent with a constant rate of increase in oxygen along with the analytical precision determined from deep oxygen measurements. If the data set is extended to September, then the Kolmogorov–Smirnov test fails ($P = 0.06$ for 2003 and 2004, with no August or September data in 2005) because of the late summer blooms. This confirms that we do detect episodic events when they are present. There is no evidence that episodic events at a frequency lower than the float cycle contribute to the oxygen increase before the late summer blooms. Aperiodic increases in oxygen concentration have been reported over 2–3-month intervals with oxygen sensors at 50 m depth, near the top of the SOM, on a mooring deployed near the HOT site[18]. Similar variability is produced in the data from float 0894 by small vertical excursions in the sharp oxygen gradient at the top of the SOM (Fig. 2a), as documented by simultaneous density variations (Fig. 2b); these are not episodic production events. If there is an episodic component to NCP, it must occur at intervals that are equal to or shorter than the float cycle period. Such a process would be more nearly periodic than episodic. We conclude that the float oxygen data provide unambiguous evidence that the euphotic zones in the North and South Pacific subtropical gyres are net producers of oxygen. Infrequent, episodic events are not required to sustain positive NCP.

METHODS SUMMARY

The data were collected with Webb Research Apex profiling floats constructed at the University of Washington. These floats were parked at 1,000 m depth and ascended to the surface at ten-day intervals. Seabird SBE43 sensors measured oxygen concentrations at 50 depths during the ascent. The oxygen data analysed here consist of the raw, transmitted values and have not been adjusted in any way.

Full Methods and any associated references are available in the online version of the paper at www.nature.com/nature.

1. del Giorgio, P. A. & Duarte, C. M. Respiration in the open ocean. *Nature* **420**, 379–384 (2002).
2. Karl, D. M., Laws, E. A., Morris, P., Williams, P. J., le B. & Emerson, S. Metabolic balance in the open sea. *Nature* **426**, 32 (2003).
3. del Giorgio, P. A., Cole, J. J. & Cimbleris, A. Respiration rates in bacteria exceed phytoplankton production in unproductive aquatic systems. *Nature* **385**, 148–151 (1997).
4. Duarte, C. M. & Agusti, S. The CO_2 balance of unproductive aquatic ecosystems. *Science* **281**, 234–236 (1998).
5. Duarte, C. M., Agusti, S., del Giorgio, P. A. & Cole, J. J. Regional carbon imbalances in the oceans. *Science* **284**, 173–174 (1999).
6. Williams, P. J., le B., Morris, P. J. & Karl, D. M. Net community production and metabolic balance at the oligotrophic ocean site, station ALOHA. *Deep-Sea Res. I* **51**, 1563–1578 (2004).
7. Williams, P. J., le B. & Bowers, D. G. Regional carbon imbalances in the oceans. *Science* **284**, 173–174 (1999).
8. Roemmich, D., Riser, S., Davis, R. & Desaubies, Y. Autonomous profiling floats: workhorse for broad-scale observations. *Mar. Technol. Soc. J.* **38**, 21–29 (2004).
9. Roemmich, D. *et al.* in *Observing the Oceans in the 21st Century* (eds Koblinsky, K. & Smith, N.) 248–258 (Australian Bureau of Meteorology, Melbourne, Australia, 2001).
10. Kortzinger, A., Schimanski, J., Send, U. & Wallace, D. The ocean takes a deep breath. *Science* **306**, 1337 (2004).
11. Johnson, K. S., Needoba, J. A., Riser, S. C. & Showers, W. J. Chemical sensor networks for the aquatic environment. *Chem. Rev.* **107**, 623–640 (2007).
12. Schulenberger, E. & Reid, J. L. The Pacific shallow oxygen maximum, deep chlorophyll maximum, and primary productivity reconsidered. *Deep-Sea Res. A* **28**, 901–919 (1981).
13. Anderson, L. A. On the hydrogen and oxygen content of marine phytoplankton. *Deep-Sea Res. I* **42**, 1675–1680 (1995).
14. Letelier, R. M., Karl, D. M., Abbott, M. R. & Bidigare, R. R. Role of late winter mesoscale events in the biogeochemical variability of the upper water column of the North Pacific Subtropical Gyre. *J. Geophys. Res.* **105**, 28723–28739 (2000).
15. Keeling, C. D., Brix, H. & Gruber, N. Seasonal and long-term dynamics of the upper ocean carbon cycle at Station ALOHA near Hawaii. *Glob. Biogeochem. Cycles* **18**, doi:10.1029/2004GB002227 (2004).
16. Behrenfeld, M. J., Boss, E., Siegel, D. A. & Shea, D. M. Carbon-based ocean productivity and phytoplankton physiology from space. *Glob. Biogeochem. Cycles* **19**, doi:10.1029/2004GB002299 (2005).
17. Scharek, R., Tupas, L. M. & Karl, D. M. Diatom fluxes to the deep sea in the oligotrophic North Pacific gyre at Station Aloha. *Mar. Ecol. Prog. Ser.* **182**, 55–67 (1999).
18. Emerson, S., Stump, C., Johnson, B. & Karl, D. M. In situ determination of oxygen and nitrogen dynamics in the upper ocean. *Deep-Sea Res. I* **49**, 941–952 (2002).
19. Schlitzer, R. Ocean Data View ⟨http://odv.awi.de⟩ (2006).

Author Contributions S.C.R. originated the idea of putting oxygen sensors on profiling floats, and directed the construction and deployment of the floats as part of the international Argo project. K.S.J. performed the data analysis. Both authors contributed to the writing of the manuscript.

Author Information All float data are available from the global Argo data center at ftp://usgodael.fnmoc.navy.mil/pub/outgoing/argo/. Reprints and permissions information is available at www.nature.com/reprints. Correspondence and requests for materials should be addressed to S.C.R. (riser@ocean.washington.edu) or K.S.J. (johnson@mbari.org).

nature

METHODS

Nearly 3,000 profiling floats are now deployed in the ocean as part of Argo[9], and about 70 of them have been equipped with sensors for dissolved oxygen[10,11]. Here we use oxygen concentrations that were measured over the course of three years by University of Washington floats 0894 (WMO Number 4900093) and 1326 (WMO Number 5900420). Oxygen concentration, temperature, salinity and pressure were measured on the ascent at 50 depths between 1,000 m and 7 m, and the data were transmitted to shore while the floats were at the surface. On every fourth profile, the floats descended to 2,000 m depth before profiling to the surface, and measurements were made at 70 depths to the surface. The floats then descended to their parking depth and drifted before returning to the surface to repeat the cycle at ten-day intervals.

Oxygen concentrations were measured on both floats with Seabird SBE43 sensors for dissolved oxygen. The SBE43 oxygen sensor is in the flow stream that is fed by the conductivity sensor pump, where it is protected from biofouling by the Seabird conductivity-cell antifouling system. This results in exceptional long-term stability that can be quantified from the variability of oxygen concentrations measured in the deep waters sampled over three years on the profiles from 2,000 m (Supplementary Fig. 1a, b). During the ten-day interval between profiles, oxygen is depleted around the sensor because it is always polarized and consuming oxygen. The oxygen sensor on float 1326 did not have sufficient time, after pump turn-on, to respond to the ambient oxygen concentration, and its initial measurements at 2,000 m were biased low. Stability of the sensor on float 1326 was quantified at 1,900 m depth. We assessed sensor performance on float 894 at 1,800 m depth, which coincides with a standard depth for oxygen measurements at the HOT time series station.

The concentration of oxygen measured by float 894 at 1,800 m over three years averages $70.8 \pm 1.3 \, \mu mol \, kg^{-1}$ (mean $\pm$ s.d., $n = 25$; Supplementary Fig. 1a). Equivalent precision is obtained for data from 2,000 m. During the same period, oxygen concentrations measured by Winkler titration in discrete samples from 1,800 m in the HOT time series averaged $79.0 \pm 2.1 \, \mu mol \, kg^{-1}$ ($n = 31$; Supplementary Fig. 1a). The oxygen measured at 1,900 m by float 1326 averaged $145.9 \pm 1.5 \, \mu mol \, kg^{-1}$ ($n = 26$) over three years (Supplementary Fig. 1b). There was a shift in water mass structure at shallower depths, as float 1326 drifted south, resulting in a bifurcation in the plot of deep oxygen against density (Fig. 1d). This same bifurcation is seen in the temperature–salinity plot (not shown). It is also seen in data from the same region on the World Ocean Circulation Experiment P17 survey, which was a meridional section along

135° W. The results for both sensors demonstrate that the precision (1 s.d.) and stability of the dissolved oxygen measurements over three years are better than $1.5 \, \mu mol \, kg^{-1}$.

As further evidence of the stability of the sensors, we consider data for oxygen concentration against time at 200 m depth, which lies below the euphotic zone. During the three-year period over which float 0894 operated (Supplementary Fig. 1c) the change in oxygen at 200 m was smaller than $-0.1 \, \mu mol \, kg^{-1} \, yr^{-1}$. Float 1326 did detect a slight upward trend over time ($1.9 \, \mu mol \, kg^{-1} \, yr^{-1}$) at 200 m (Supplementary Fig. 1d), which was paralleled by an equivalent trend in oxygen solubility[20] as the float drifted south; again, the sensor appeared stable. However, the variability in oxygen concentrations at 200 m depth was much larger than that found at depths below 1,000 m (Supplementary Fig. 1a, b) or near the surface (Supplementary Fig. 2). Oxygen concentrations determined by Winkler titration at 200 m in the HOT time series over the same period ($197 \pm 6 \, \mu mol \, kg^{-1}$) have similar variability to the float data ($188 \pm 6 \, \mu mol \, kg^{-1}$; Supplementary Fig. 1c). The high variability at 200 m must reflect real changes in oxygen concentration driven by physical and biological processes, and it does not reflect sensor precision.

Variability in oxygen concentration within the mixed layer primarily reflects changes in oxygen solubility (Supplementary Fig. 2a, b). As the water column warms during spring and summer, oxygen solubility[20] decreases and the oxygen in the mixed layer outgasses to the atmosphere. Although the float data suggest that concentration of oxygen in the mixed layer averages $10 \, \mu mol \, kg^{-1}$ (float 0894) and $16 \, \mu mol \, kg^{-1}$ (float 1326) below the concurrent solubility values (Fig. 2a, b), these differences probably reflect inaccuracies in the absolute calibration of the oxygen sensors. Measurements of near-surface oxygen generally indicate a supersaturation of 0 to $+4 \, \mu mol \, kg^{-1}$, particularly near the HOT site[18]. Similar offsets in the calibration of the sensor on float 0894 are seen at 200 and 1,800 m when compared with the Winkler titration data at the HOT site (Supplementary Figs 1c and 2a).

Despite the calibration offsets, the inherent noise and drift of the oxygen sensors are less than one-tenth of the annual changes in oxygen detected in the SOM. To exploit this high precision, here we concern ourselves with relative changes in the concentration of oxygen over time rather than the absolute accuracy of the oxygen sensor.

20. Weiss, R. F. The solubility of nitrogen, oxygen and argon in water and seawater. *Deep-Sea Res. A* **17**, 721–735 (1970).